Navigator-gated 3D Cine DENSE MRI of the Left Ventricle

X. Zhong[1,2], C. H. Meyer[1,3], C. M. Kramer[3], and F. H. Epstein[1,3]

[1]Biomedical Engineering, University of Virginia, Charlottesville, VA, United States, [2]MR R&D Collaborations, Siemens Medical Solutions, Atlanta, GA, United States, [3]Radiology, University of Virginia, Charlottesville, VA, United States

Introduction. Heart disease can affect any region of the myocardium, and the complex movement and contraction of the heart occurs in a three-dimensional (3D) pattern. Thus, imaging of cardiac function should ideally cover the entire heart and completely quantify myocardial deformation in 3D. The purposes of the present study were to (a) develop a free-breathing navigator-gated 3D cine DENSE (Displacement-ENcoding with Stimulated Echoes (1,2)) pulse sequence to acquire such data and (b) implement post-processing methods to quantify 3D myocardial strain throughout the left ventricle (LV).

Methods. An ECG-gated segmented spiral cine DENSE pulse sequence (3) was modified to acquire 3D data and perform online image reconstruction on a 1.5T MRI scanner (Siemens Avanto, Erlangen, Germany). A 3D stacked-spiral k-space trajectory was employed for rapid data acquisition. Three-point phase cycling was used for artifact suppression (4), a balanced four-point method was used for optimal displacement encoding (5), and field map acquisition and online spiral deblurring were employed (6). A navigator echo (7) was placed at the end of the cardiac cycle, so as not to interfere with imaging of the onset of myocardial contraction. The navigator echo was used to accept or reject the DENSE data acquired in the subsequent heart beat. Five normal volunteers provided informed consent and were studied in accordance with protocols approved by our institutional review board. Imaging parameters included voxel size = 2.8 × 2.8 × 5.0 mm^3, flip angle = 20°, TR = 16 ms, TE = 1.3 ms, number of spiral interleaves = 6, temporal resolution = 32 ms, and cardiac phases = 22. A double-oblique 3D volume was aligned with the short and long axes of the LV. Fourteen k-space partitions were acquired and then zero-padded to reconstruct 28 slices. A 3-mm navigator acceptance window was placed at the end-expiration position. For displacement and strain analysis, images were exported and processed offline using a Matlab program which extended previous analysis 2D methods (8) to 3D. Specifically, the LV was manually segmented and automatically phase unwrapped. Tissue tracking was performed by scattered data interpolation using radial basis functions (RBF) (9). The strain tensor was calculated using finite strain theory (10), and was decomposed into radial (E_{rr}), circumferential (E_{cc}) and longitudinal (E_{ll}) directions of the local LV coordinate system (11). To validate the 3D measurements, multiple 2D cine DENSE acquisitions were performed in short- and long-axis planes. Non-navigator-gated 3D data were also acquired in some volunteers.

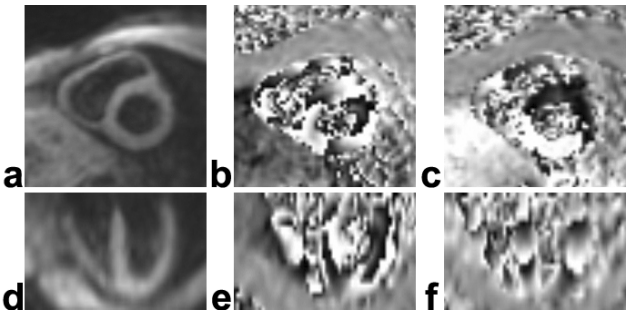

Fig. 1 Example magnitude- (a,d) and phase-reconstructed (b,c,e,f) images of 3D spiral cine DENSE data at end-systole. The slice orientation of this 3D acquisition is parallel to short-axis planes. (a) is the mid-level short-axis magnitude image. (b) and (c) are the corresponding phase images with displacement encoded in the horizontal and through-plane directions, respectively. (d) is the magnitude image of the long-axis four-chamber view extracted from the corresponding online short-axis 3D data. (e) and (f) are the corresponding reconstructed phase images with displacement encoded in the horizontal and vertical directions, respectively.

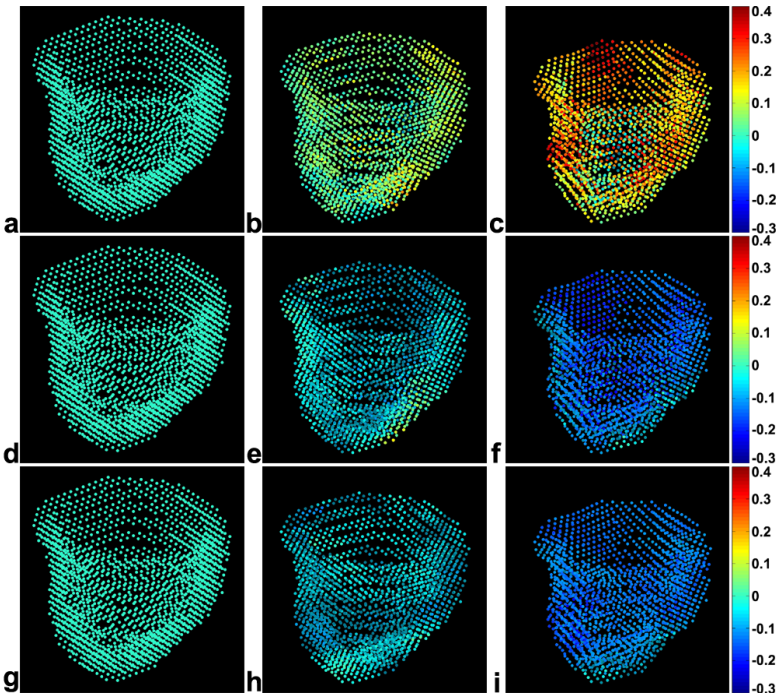

Fig. 2 Example E_{rr} (a-c), E_{cc} (d-f) and E_{ll} (g-i) strains computed throughout the LV. Data are shown at end-diastole (a,d,g), mid-systole (b,e,h) and end-systole (c,f,i). Dots represent voxel positions, while color represents strain.

Results. The acceptance rate of the navigator was 48.0 ± 15.7%, and the total scan time was 20.5 ± 5.7 minutes. High-quality data were acquired from all volunteers, and comparisons with non-navigator-gated free breathing scans clearly demonstrated the reduction of respiratory artifacts provided by navigator gating. Example magnitude-reconstructed and the corresponding phase-reconstructed 3D DENSE images at end-systole are shown in Fig. 1. Typical 3D strain data from one subject are shown in Fig. 2, where the development of E_{rr} (a-c), E_{cc} (d-f), and E_{ll} strain (g-i) from end diastole (a,d,g) through mid systole (b,e,h) to end systole (c,f,i) are displayed for the entire LV. Strain values and strain-time curves were consistent with previous data from myocardial tagging and DENSE studies of normal volunteers. For the comparison with 2D cine DENSE, linear regression showed that radial, circumferential, and longitudinal strains from 3D cine DENSE correlated well with those from 2D cine DENSE, with a slope of 0.974 and R = 0.647 for E_{rr}, a slope of 0.945 and R = 0.902 for E_{cc}, and a slope of 0.888 and R = 0.772 for E_{ll}. Bland-Altman analysis also demonstrated good agreement between 2D and 3D cine DENSE methods for all 3 strains.

Conclusion. A free-breathing navigator-gated 3D spiral cine DENSE pulse sequence and the corresponding data analysis algorithms were developed that provide high spatial and temporal resolutions, coverage of the entire LV, and measurement of 3D strain with a scan time of approximately 20 minutes. In normal volunteers, the resulting strain data show good agreement with those from 2D cine DENSE. With additional development aimed at further shortening the scan time and automating image analysis, these methods may enable routine clinical imaging that completely quantifies contractile function throughout the LV in patients with contractile dysfunction.

Acknowledgements. Supported by NIBIB grant RO1 EB 001763 and Siemens Medical Solutions.

1. Aletras et al. JMR 1999;137:247-252.
2. Kim et al. Radiology 2004;230:862-871.
3. Zhong et al. 15th ISMRM 2007;3599.
4. Callot et al. MRM 2003;50:531-540.
5. Zhong et al. MRM. In press.
6. Irrarazabal et al. MRM 1996;35:278-282.
7. Taylor et al. JMRI 1997;7:629-636.
8. Spottiswoode et al. IEEE-TMI 2007;26:15-30.
9. Hardy. JGR 1971;176:1905-1915.
10. Young et al. Radiology 1992;185:241-247.
11. Moore et al. Radiology 2000;214:453-466.